Appl. Math. Mech. -Engl. Ed., **43**(3), 327–340 (2022)

APPLIED MATHEMATICS AND MECHANICS (ENGLISH EDITION)

https://doi.org/10.1007/s10483-022-2824-7

Propagation of Rayleigh-type surface waves in a layered piezoelectric nanostructure with surface effects*

Lele ZHANG[1,2], Jing ZHAO[3], Guoquan NIE[1,2], Jinxi LIU[1,2,†]

1. State Key Laboratory of Mechanical Behavior and System Safety of Traffic Engineering Structures, Shijiazhuang Tiedao University, Shijiazhuang 050043, China;
2. Hebei Key Laboratory of Mechanics of Intelligent Materials and Structures, Department of Engineering Mechanics, Shijiazhuang Tiedao University, Shijiazhuang 050043, China;
3. Department of Architecture, Shijiazhuang Institute of Railway Technology, Shijiazhuang 050041, China

(Received Sept. 8, 2021 / Revised Dec. 20, 2021)

Abstract This work investigates the dispersion properties of Rayleigh-type surface waves propagating in a layered piezoelectric nanostructure composed of a piezoelectric nanofilm over an elastic substrate. As one of the most important features of nanostructures, surface effects characterized by surface stresses and surface electric displacements are taken into account through the surface piezoelectricity theory and the nonclassical mechanical and electrical boundary conditions. Concrete expressions of the dispersion equation are derived, and numerical results are provided to examine the effects of several surface-related parameters, including the surface elasticity, surface piezoelectricity, surface dielectricity, surface density, as well as surface residual stress, on the dispersion modes and phase velocity. The size-dependent dispersion behaviors occurring with surface effects are also predicted, and they may vanish once the thickness of the piezoelectric nanofilm reaches a critical value.

Key words surface effect, surface piezoelectricity, dispersion behavior, piezoelectric nanofilm, Rayleigh wave

Chinese Library Classification O353
2010 Mathematics Subject Classification 74J15

1 Introduction

Piezoelectric nanomaterials have many unique properties, such as enhanced electromechanical coupling[1–2], low power dissipation[3–4], and sensitive response[5–6]. These advantages make them strong candidates as building blocks and functional elements for applications in

* Citation: ZHANG, L. L., ZHAO, J., NIE, G. Q., and LIU, J. X. Propagation of Rayleigh-type surface waves in a layered piezoelectric nanostructure with surface effects. *Applied Mathematics and Mechanics* (*English Edition*), **43**(3), 327–340 (2022) https://doi.org/10.1007/s10483-022-2824-7

† Corresponding author, E-mail: liujx02@hotmail.com

Project supported by the National Natural Science Foundation of China (Nos. 11802185 and 11872041), the Natural Science Foundation of Hebei Province of China (No. A2019210203), and the Youth Fund Project of Hebei Education Department of China (No. QN2018037)

the nanoelectromechanical systems (NEMSs), which mainly include generators[4], sensors[5–6], resonators[7–8], transistors[9], and diodes[10] at the nanoscale. With the rapid development of nanotechnology, many piezoelectric nanomaterials have been fabricated in a wide range of shapes and geometries. Typical examples are zero-dimensional nanoparticles, one-dimensional nanowires, and two-dimensional nanofilms and nanoribbons. Among the above-mentioned nanodevices, piezoelectric nanofilms are commonly used to be key components. Therefore, to improve the performance of these novel devices, it is necessary to understand the mechanical and physical behaviors of nanostructures involving piezoelectric nanofilms.

Previous studies have demonstrated that once the size of piezoelectric structures is down to nanoscale, their overall mechanical properties often differ markedly from the macroscopic counterparts[11–18]. Due to the high ratio of surface to bulk volume at nanoscale, surface effects are regarded as one of the major factors to these exceptional behaviors. To date, increased efforts, including experimental measurements[11–12], atomistic simulations[13–14], and theoretical predictions[15–18], have been devoted to investigating the influence of surface effects on the mechanical behaviors of piezoelectric nanostructures. Since controlled experiments on nanomaterials are extremely difficult and atomistic simulations are time consuming in computation, theoretical modelling is naturally pursued as an alternative and cost-effective method by many researchers. Assuming that a surface is a two-dimensional continuum of vanishing thickness which possesses own material properties different from those of their bulk counterparts, Gurtin and Murdoch[19] proposed the well-known surface elasticity model. The proposed model has been successfully used to predict the size-dependent properties of many elastic nanostructures[20]. Inspired by this model, Huang and Yu[21] and Pan et al.[22] carried out pioneering work in developing the surface piezoelectricity theory to account for the surface effects of piezoelectric nanomaterials. Subsequently, it was widely adopted to conduct static and dynamic analyses of various piezoelectric nanostructures, such as the effective properties of piezoelectric nanocomposites[23], the dynamic strength of a piezoelectric nanoparticle[24], the wave characteristics of piezoelectric nanoplates[25–26], the bending of piezoelectric nanowires[27], the vibration and buckling of piezoelectric nanobeams and nanofilms[28–30], and the wrinkling of piezoelectric nanofilms[31]. More applications based on the surface piezoelectricity theory can refer to a comprehensive review given by Yan and Jiang[17]. Very recently, Guo and Wei[32] extended the surface piezoelectricity model to study the propagation properties of in-plane elastic waves in a nanoscale N-type piezoelectric semiconductor/piezoelectric dielectric layered periodic composite.

Thin film surface acoustic wave (SAW) devices including sensors, filters, and delay lines, which often consist of a piezoelectric thin film deposited on a non-piezoelectric substrate, are considered as the basic components employed in various electromechanical systems for signal processing and sensing. The design of such devices is mainly based on the propagation modes of Love or Rayleigh-type surface waves according to the difference in working mechanisms. For instance, in the field of biosensing, Rayleigh wave devices are preferentially used for the detection of gas-phase samples while Love wave devices are generally used for liquid-phase ones[33]. At present, the rapid development of NEMSs requires the characteristic size of components to be reduced to nanoscale. Therefore, understanding the propagation characteristics of surface waves in thin film SAW nanodevices is of practical importance for their design and applications. For Love surface waves in a piezoelectric nanofilm/elastic substrate structure, Yang et al.[34] and Wang et al.[35] investigated the dispersion behaviors with the consideration of flexoelectric effects and surface effects, respectively. However, the relevant literature for Rayleigh-type surface waves is very limited so far. To further enrich the studies on wave properties of thin film SAW nanodevices, this work aims to present the size-dependent dispersion characteristics of Rayleigh-type surface waves propagating in a layered piezoelectric nanostructure by considering the surface effects. Within the framework of the surface piezoelectricity theory, concrete expressions of the dispersion equation will be derived to show how the surface material properties

and surface residual stress change the dispersion modes and phase velocity.

2 Problem formulation

A layered nanostructure composed of an h-thick piezoelectric nanofilm perfectly bonded to an elastic substrate is shown in Fig. 1, where the substrate is treated as a half-space since its thickness is much larger compared with the film. With reference to a spatial rectangular coordinate system $x_1x_2x_3$, the layered structure is assumed to be infinite in the x_1x_2-plane, and the surface layer at $x_3 = h$ is denoted by Γ. The piezoelectric nanofilm poling along the x_3-axis is homogeneous and transversely isotropic. Here, we consider the deformation in plane strain (x_2x_3-plane), all field variables are independent of x_1, and only the in-plane displacements u_i $(i = 2, 3)$ exist. Therefore, in the absence of body forces and volume electric charges, the dynamic and charge equilibrium equations for the piezoelectric nanofilm can be written as

$$c_{11}u_{2,22} + c_{44}u_{2,33} + (c_{13} + c_{44})u_{3,23} + (e_{31} + e_{15})\phi_{,23} = \rho\ddot{u}_2, \tag{1}$$

$$(c_{44} + c_{13})u_{2,23} + c_{44}u_{3,22} + c_{33}u_{3,33} + e_{15}\phi_{,22} + e_{33}\phi_{,33} = \rho\ddot{u}_3, \tag{2}$$

$$(e_{15} + e_{31})u_{2,23} + e_{15}u_{3,22} + e_{33}u_{3,33} - \kappa_{11}\phi_{,22} - \kappa_{33}\phi_{,33} = 0, \tag{3}$$

where c, e, and κ are, respectively, the elastic, piezoelectric, and dielectric constants, ϕ is the electric potential, and ρ is the mass density of the nanofilm; the subscripted comma indicates the derivative with respect to the spatial coordinate that follows, and the superimposed dot denotes the derivative with respect to time t.

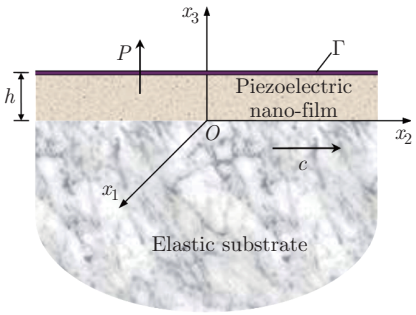

Fig. 1 Geometry and coordinate systems of problem (color online)

For time-harmonic wave motion, the solutions to Eqs. (1)–(3) representing a standing wave in the x_3-direction and a propagating wave in the x_2-direction should take the following forms:

$$u_2 = A_1 \mathrm{e}^{kbx_3}\mathrm{e}^{\mathrm{i}k(x_2 - ct)}, \tag{4}$$

$$u_3 = A_2 \mathrm{e}^{kbx_3}\mathrm{e}^{\mathrm{i}k(x_2 - ct)}, \tag{5}$$

$$\phi = A_3 \mathrm{e}^{kbx_3}\mathrm{e}^{\mathrm{i}k(x_2 - ct)}, \tag{6}$$

where A_i $(i = 1, 2, 3)$ are amplitudes, b is an unknown parameter to be determined, k is the wave number, c is the phase velocity, and ω $(= kc)$ is the circular frequency.

Substituting Eqs. (4)–(6) into Eqs. (1)–(3) yields the following homogeneous equations:

$$\boldsymbol{M}\boldsymbol{A} = \boldsymbol{0}, \tag{7}$$

in which $\boldsymbol{A} = (A_1 \;\; A_2 \;\; A_3)^{\mathrm{T}}$, and $\boldsymbol{M}$ is a symmetric matrix whose elements are given by

$$\begin{cases} M_{11} = c_{44}b^2 - c_{11} + \rho c^2, \quad M_{12} = M_{21} = (c_{13} + c_{44})b\mathrm{i}, \quad M_{13} = M_{31} = (e_{31} + e_{15})b\mathrm{i}, \\ M_{22} = c_{33}b^2 - c_{44} + \rho c^2, \quad M_{23} = M_{32} = e_{33}b^2 - e_{15}, \quad M_{33} = \kappa_{11} - \kappa_{33}b^2. \end{cases} \tag{8}$$

To get nontrivial solutions to Eq. (7), the determinant of the coefficient matrix $\boldsymbol{M}$ must be equal to zero, which results in a cubic equation in b^2 as

$$\chi_3 b^6 + \chi_2 b^4 + \chi_1 b^2 + \chi_0 = 0, \tag{9}$$

where the detailed expressions of χ_j $(j = 0, 1, 2, 3)$ are

$$\begin{cases} \chi_3 = -c_{44}(c_{33}\kappa_{33} + e_{33}^2), \\ \chi_2 = c_{33}(c_{44}\kappa_{11} + (e_{31} + e_{15})^2) + \kappa_{33}(c_{44}(c_{44} - \rho c^2) + c_{33}(c_{11} - \rho c^2) - (c_{13} + c_{44})^2) \\ \qquad + 2e_{33}(c_{44}e_{15} - (c_{13} + c_{44})(e_{31} + e_{15})) + e_{33}^2(c_{11} - \rho c^2), \\ \chi_1 = -\kappa_{33}(c_{11} - \rho c^2)(c_{44} - \rho c^2) - c_{44}e_{15}^2 \\ \qquad - \kappa_{11}(c_{44}(c_{44} - \rho c^2) + c_{33}(c_{11} - \rho c^2) - (c_{13} + c_{44})^2) \\ \qquad - 2e_{15}(e_{33}(c_{11} - \rho c^2) - (c_{13} + c_{44})(e_{31} + e_{15})) - (e_{31} + e_{15})^2(c_{44} - \rho c^2), \\ \chi_0 = (c_{11} - \rho c^2)(e_{15}^2 + \kappa_{11}(c_{44} - \rho c^2)). \end{cases} \tag{10}$$

For a given value of c, there exist three pairs of b by solving Eq. (9), and each of b represents an independent solution to the partial differential equations (1)–(3). As a consequence, the mechanical displacements and electric potential in the piezoelectric nanofilm should be further expressed in the form of linear combination, i.e.,

$$u_2 = \sum_{m=1}^{6} \hbar_m A_{3m} \mathrm{e}^{kb_m x_3} \mathrm{e}^{\mathrm{i}k(x_2 - ct)}, \tag{11}$$

$$u_3 = \sum_{m=1}^{6} \overline{\lambda}_m A_{3m} \mathrm{e}^{kb_m x_3} \mathrm{e}^{\mathrm{i}k(x_2 - ct)}, \tag{12}$$

$$\phi = \sum_{m=1}^{6} A_{3m} \mathrm{e}^{kb_m x_3} \mathrm{e}^{\mathrm{i}k(x_2 - ct)}, \tag{13}$$

where $\hbar_m$ and $\overline{\lambda}_m$ are the amplitude ratios that can be defined from Eq. (7) as

$$\begin{cases} \hbar_m = \dfrac{A_{1m}}{A_{3m}} = \dfrac{M_{12}M_{23} - M_{13}M_{22}}{M_{11}M_{22} - M_{12}M_{21}}, \\ \overline{\lambda}_m = \dfrac{A_{2m}}{A_{3m}} = \dfrac{M_{13}M_{21} - M_{11}M_{23}}{M_{11}M_{22} - M_{12}M_{21}}. \end{cases} \tag{14}$$

Setting

$$\begin{cases} c_{11} = c_{33} = \lambda + 2\mu, \quad c_{13} = \lambda, \quad c_{44} = \mu, \\ e_{31} = e_{15} = e_{33} = 0, \quad \kappa_{11} = \kappa_{33} = \eta \end{cases} \tag{15}$$

in Eqs. (1)–(3) yields the governing equations for the elastic substrate as follows:

$$(\lambda + 2\mu)\breve{u}_{2,22} + \mu\breve{u}_{2,33} + (\lambda + \mu)\breve{u}_{3,23} = \breve{\rho}\ddot{\breve{u}}_2, \tag{16}$$

$$(\lambda + \mu)\breve{u}_{2,23} + \mu\breve{u}_{3,22} + (\lambda + 2\mu)\breve{u}_{3,33} = \breve{\rho}\ddot{\breve{u}}_3, \tag{17}$$

$$\nabla^2\breve{\phi} = 0, \tag{18}$$

where λ and μ are Lamé's elastic constants, η is the dielectric coefficient of the substrate, and $\nabla^2 = \frac{\partial^2}{\partial x_2^2} + \frac{\partial^2}{\partial x_3^2}$ is the two-dimensional Laplacian operator. To distinguish from the quantities in the piezoelectric nanofilm, the overline is adopted to denote the elastic substrate.

Similar to Eqs. (4)–(6), we consider the solutions to Eqs. (16)–(18) with the following forms:

$$\breve{u}_2 = \breve{A}_1 \mathrm{e}^{k\breve{b}x_3}\mathrm{e}^{\mathrm{i}k(x_2-ct)}, \tag{19}$$

$$\breve{u}_3 = \breve{A}_2 \mathrm{e}^{k\breve{b}x_3}\mathrm{e}^{\mathrm{i}k(x_2-ct)}, \tag{20}$$

$$\breve{\phi} = \breve{A}_3 \mathrm{e}^{k\breve{b}x_3}\mathrm{e}^{\mathrm{i}k(x_2-ct)}. \tag{21}$$

Substituting Eq. (21) into Eq. (18) easily yields $\breve{b} = \pm 1$. In view of the condition $\lim\limits_{x_3\to-\infty}\breve{\phi} = 0$, it is required that $\breve{b} = 1$. Thus, the electric potential in the elastic substrate may be rewritten as

$$\breve{\phi} = \breve{A}_3 \mathrm{e}^{kx_3}\mathrm{e}^{\mathrm{i}k(x_2-ct)}. \tag{22}$$

Then, substituting Eqs. (19)–(20) into Eqs. (16)–(17) gives

$$\boldsymbol{N}\breve{\boldsymbol{A}} = \boldsymbol{0}, \tag{23}$$

where $\breve{\boldsymbol{A}} = (\breve{A}_1 \quad \breve{A}_2)^{\mathrm{T}}$, and the coefficient matrix $\boldsymbol{N}$ is defined as

$$\begin{cases} N_{11} = \mu\breve{b}^2 - (\lambda+2\mu) + \breve{\rho}c^2, \quad N_{12} = N_{21} = (\lambda+\mu)\breve{b}\mathrm{i}, \\ N_{22} = (\lambda+2\mu)\breve{b}^2 - \mu + \breve{\rho}c^2. \end{cases} \tag{24}$$

The existence of nontrivial solutions for $\breve{A}$ requires $|\boldsymbol{N}| = 0$, which can be further expanded as

$$\varsigma_2\breve{b}^4 + \varsigma_1\breve{b}^2 + \varsigma_0 = 0, \tag{25}$$

in which

$$\begin{cases} \varsigma_2 = \mu(\lambda+2\mu), \quad \varsigma_1 = -2\mu(\lambda+2\mu) + (\lambda+3\mu)\breve{\rho}c^2, \\ \varsigma_0 = \mu(\lambda+2\mu) - (\lambda+3\mu-\breve{\rho}c^2)\breve{\rho}c^2. \end{cases} \tag{26}$$

Four roots for b can be solved from Eq. (25), and their forms are closely dependent on the range of wave velocity c. For Rayleigh-type surface wave, $c < \breve{c}_{\mathrm{sh}}$ should be satisfied to ensure that all the solutions of b are real numbers. Two positive b are retained since the displacement amplitude may decay as the depth increases. Accordingly, the complete expressions of displacement fields in the elastic substrate are given as

$$\breve{u}_2 = \sum_{n=1}^{2} \ell_n \breve{A}_{2n} \mathrm{e}^{k\breve{b}_n x_3}\mathrm{e}^{\mathrm{i}k(x_2-ct)}, \tag{27}$$

$$\breve{u}_3 = \sum_{n=1}^{2} \breve{A}_{2n} \mathrm{e}^{k\breve{b}_n x_3}\mathrm{e}^{\mathrm{i}k(x_2-ct)}, \tag{28}$$

where $\ell_n = \frac{\breve{A}_{1n}}{\breve{A}_{2n}} = -\frac{N_{12}}{N_{11}}$ is the amplitude ratio.

3 Derivation of dispersion equation

Within the framework of surface piezoelectricity theory, the surface stresses and the surface electric displacements related to the material properties near the surface are introduced to depict the surface effects, which actually results in the nonclassical mechanical and electrical

boundary conditions. As the current formulation is of x_2x_3-plane strain nature, the boundary conditions at the surface Γ are provided as[25,36]

$$\sigma^{\mathrm{s}}_{22,2} - \sigma_{23} = \rho_{\mathrm{s}}\ddot{u}_2, \quad x_3 = h, \tag{29}$$

$$\sigma_0 u_{3,22} - \sigma_{33} = \rho_{\mathrm{s}}\ddot{u}_3, \quad x_3 = h, \tag{30}$$

$$D^{\mathrm{s}}_{2,2} - D_3 = 0, \quad x_3 = h, \tag{31}$$

where σ_0 and ρ_{s} are, respectively, the residual stress and mass density of the surface. The stress tensors σ_{23}, σ_{33}, and the electric displacement vector D_3 for the piezoelectric bulk are given by

$$\sigma_{23} = c_{44}(u_{2,3} + u_{3,2}) + e_{15}\phi_{,2}, \tag{32}$$

$$\sigma_{33} = c_{13}u_{2,2} + c_{33}u_{3,3} + e_{33}\phi_{,3}, \tag{33}$$

$$D_3 = e_{31}u_{2,2} + e_{33}u_{3,3} - \kappa_{33}\phi_{,3}. \tag{34}$$

Following the surface piezoelectricity constitutive relations[21–22], the surface stress σ^{s}_{22} and the surface electric displacement D^{s}_2 obey

$$\sigma^{\mathrm{s}}_{22} = \sigma_0 + c^{\mathrm{s}}_{11}u_{2,2} + e^{\mathrm{s}}_{31}\phi_{,3}, \quad x_3 = h, \tag{35}$$

$$D^{\mathrm{s}}_2 = D_0 - \kappa^{\mathrm{s}}_{11}\phi_{,2}, \quad x_3 = h, \tag{36}$$

where D_0 is the residual surface electric displacement, and c^{s}_{11}, e^{s}_{31}, and κ^{s}_{11} are the surface elastic, surface piezoelectric, and surface dielectric constants, respectively. In principle, the precise values of surface material constants can be obtained from detailed atomistic simulations and experiments. However, to date, only few of them are available for piezoelectric nanomaterials due to lack of such work. To qualitatively evaluate the surface effects on the mechanical responses of piezoelectric nanostructures, an approximate but reasonable method is generally used to describe the surface material properties[22]. It assumes that each surface material constant can merely be expressed as the scaled versions of its bulk counterpart through a characteristic length at the nanoscale. For the present case,

$$c^{\mathrm{s}}_{11} = f_c c_{11}, \quad e^{\mathrm{s}}_{31} = f_e e_{31}, \quad \kappa^{\mathrm{s}}_{11} = f_\kappa \kappa_{11}, \quad \rho_{\mathrm{s}} = f_\rho \rho, \tag{37}$$

where f_c, f_e, f_κ, and f_ρ are the characteristic lengths representing the magnitudes of surface elasticity, surface piezoelectricity, surface dielectricity, and the surface density, respectively.

To avoid the presence of too many unknown material constants in the computation, the interface effects at $x_3 = 0$ are ignored. Consider the continuity of mechanical and electric quantities along the interface, which requires

$$u_2 = \breve{u}_2, \quad u_3 = \breve{u}_3, \quad \sigma_{23} = \breve{\sigma}_{23}, \quad \sigma_{33} = \breve{\sigma}_{33}, \quad x_3 = 0, \tag{38}$$

$$\phi = \breve{\phi}, \quad D_3 = \breve{D}_3, \quad x_3 = 0, \tag{39}$$

where the mechanical stress and electric displacement in the substrate are given by

$$\breve{\sigma}_{23} = \mu(\breve{u}_{2,3} + \breve{u}_{3,2}), \tag{40}$$

$$\breve{\sigma}_{33} = \lambda\breve{u}_{2,2} + (\lambda + 2\mu)\breve{u}_{3,3}, \tag{41}$$

$$\breve{D}_3 = -\eta\breve{\phi}_{,3}. \tag{42}$$

Upon substitution of the expressions of corresponding variables, Eqs. (29)–(31) and (38)–(39) become a linear system of algebraic equations for unknown amplitudes. Then, the dispersion equation can be derived from the condition that the determinant of the coefficient matrix of the resulting algebraic equations must vanish as

$$|\boldsymbol{Q}| = 0, \tag{43}$$

where $\boldsymbol{Q}$ is a 9×9 matrix whose nonzero elements are

$$\begin{cases} Q_{1m} = (k(-c_{11}^{\mathrm{s}}\hbar_m + e_{31}^{\mathrm{s}} b_m \mathrm{i}) - c_{44}(\hbar_m b_m + \overline{\lambda}_m \mathrm{i}) - e_{15}\mathrm{i} + \rho_{\mathrm{s}} k c^2 \hbar_m) \exp(k b_m h), \\ Q_{2m} = (k\sigma_0 \overline{\lambda}_m + (c_{13}\hbar_m \mathrm{i} + c_{33}\overline{\lambda}_m b_m + e_{33} b_m) - \rho_{\mathrm{s}} k c^2 \overline{\lambda}_m) \exp(k b_m h), \\ Q_{3m} = (k\kappa_{11}^{\mathrm{s}} - e_{31}\hbar_m \mathrm{i} - e_{33}\overline{\lambda}_m b_m + \kappa_{33} b_m) \exp(k b_m h), \\ Q_{4m} = \hbar_m, \quad Q_{4(n+6)} = -\ell_n, \quad Q_{5m} = \overline{\lambda}_m, \quad Q_{5(n+6)} = -1, \\ Q_{6m} = c_{44}(\hbar_m b_m + \overline{\lambda}_m \mathrm{i}) + e_{15}\mathrm{i}, \quad Q_{6(n+6)} = -\mu(\mathrm{i} + \ell_n \breve{b}_n), \\ Q_{7m} = b_m(c_{33}\overline{\lambda}_m + e_{33}) + c_{13}\hbar_m \mathrm{i}, \quad Q_{7(n+6)} = -\lambda \ell_n \mathrm{i} - (\lambda + 2\mu)\breve{b}_n, \\ Q_{8m} = 1, \quad Q_{89} = -1, \quad Q_{9m} = b_m(e_{33}\overline{\lambda}_m - \kappa_{33}) + e_{31}\hbar_m \mathrm{i}, \quad Q_{99} = \eta. \end{cases} \tag{44}$$

It is noted that the relations between the frequency and phase velocity describing the dispersion characteristics can be obtained by solving Eq. (43). Because of the complexity, the numerical techniques are commonly adopted to find the roots of phase velocity for a given frequency.

4 Numerical results and discussion

In this section, some numerical examples are presented to examine the effects of surface properties on the dispersion characteristics of Rayleigh-type surface waves. Without loss of generality, it is assumed that the piezoelectric nanofilm and elastic substrate are made of PZT-5H and diamond, respectively. The material constants used for the numerical calculation are listed in Table 1. For the sake of brevity, the nondimensional circular frequency $K = \omega h/c_{\mathrm{sh}}$ and phase velocity c/c_{sh} are introduced in the following discussion, in which $c_{\mathrm{sh}} = \sqrt{(c_{44} + e_{15}^2/\kappa_{11})/\rho}$ is the velocity of shear bulk wave propagating in the piezoelectric medium. To be noted, we take $h = 2\,\mathrm{nm}$ and $\sigma_0 = 0\,\mathrm{N \cdot m^{-1}}$ in the following analysis unless otherwise stated.

Table 1 Material parameters used for numerical calculation[37–38]

Material constant	Symbol	PZT-5H	Diamond
Elastic constants/(10^9 N · m^{-2})	c_{11}	126	–
	c_{13}	83.9	–
	c_{33}	117	–
	c_{44}	23	–
	λ	–	86.4
	μ	–	533.3
Piezoelectric constants/(C · m^{-2})	e_{15}	17	–
	e_{31}	−6.5	–
	e_{33}	23.3	–
Dielectric constants/(10^{-11} C · V^{-1} · m^{-1})	κ_{11}	1 505	–
	κ_{33}	1 302	–
	η	–	5.02
Density/(kg · m^{-3})	ρ	7 500	3 512

Dispersion curves of the first six modes for Rayleigh-type surface waves are plotted in Fig. 2, where the piezoelectric films with and without surface effects are depicted by $f_c = 0.06\,\mathrm{nm}$, $f_e = 4.6\,\mathrm{nm}$, $f_\kappa = f_\rho = 1.0\,\mathrm{nm}$, and $f_c = f_e = f_\kappa = f_\rho = 0\,\mathrm{nm}$, respectively. It should be pointed out that the characteristic lengths $f_c = 0.06\,\mathrm{nm}$ and $f_e = 4.6\,\mathrm{nm}$ correspond to $c_{11}^{\mathrm{s}} = 7.56\,\mathrm{N \cdot m^{-1}}$ and $e_{31}^{\mathrm{s}} = -3 \times 10^{-8}\,\mathrm{C \cdot m^{-1}}$. These two surface constants as a valid approximation for PZT-5H are first provided by Huang and Yu[21], and then have been widely used in many works[25,27–31]. As can be seen from Fig. 2, the dispersion curves involving surface

effects deviate obviously from the corresponding classical case, which implies the necessity of considering the surface effects during the dispersion analysis of piezoelectric nanostructures. For Rayleigh-type surface waves propagating in the piezoelectric film/elastic substrate structure, the phase velocity of each mode decreases as the frequency increases. The 1st mode known as fundamental Rayleigh mode exists under an arbitrary frequency, as opposed to the others named high-order modes which may propagate only above particular frequencies called the cut-off frequencies. Whether with or without surface effects, it is observed that $c = \check{c}_{\mathrm{R}}$ for the 1st mode when $K \to 0$ and $c = \check{c}_{\mathrm{sh}}$ at the cut-off frequency of high-order modes, in which $\check{c}_{\mathrm{R}}$ and $\check{c}_{\mathrm{sh}}$ are the Rayleigh wave velocity and shear wave velocity of the elastic substrate, respectively. This is due to the fact that the waves mainly propagate in the semi-infinite substrate at a very low frequency, and apparently the surface effects of piezoelectric film have no impact on the wave characteristics of elastic substrate. As K grows larger, the thickness of the film becomes relatively bigger compared with the wavelength, and then the waves propagate as in a piezoelectric half-space. Hence, the phase velocity of the 1st mode is asymptotic to the Rayleigh wave velocity c_{R} of piezoelectric medium in the classical case. However, when the surface effects are considered, it no longer tends to a certain value at higher frequencies. It is therefore reasonably inferred that Rayleigh surface waves in a piezoelectric half-space with the consideration of surface effects are dispersive. This conclusion is further confirmed by Eq. (A4) in Appendix A, and the phase velocity curve based on Eq. (A4) is also plotted to compare with the 1st mode in Fig. 3. It can be clearly observed that two curves converge at a large enough value of K and then decrease continually with increasing the frequency. In addition, for the high-order modes, Fig. 2 shows that the magnitude of the cut-off frequency is changed significantly in the presence of surface effects, and the higher the order is, the greater the change becomes. The phase velocity of the other high-order modes asymptotically approaches to c_{sh} as the frequency increases except the 2nd mode with the surface effects considered, whose velocity is less than c_{sh} and does not tend to a constant at higher frequencies.

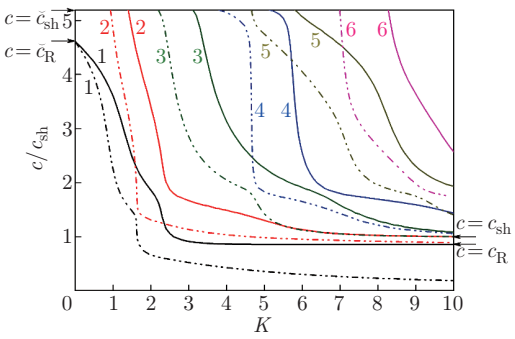

Fig. 2 Dispersion curves of first six modes for Rayleigh-type surface waves in piezoelectric film/elastic substrate structure, where dashed-dotted lines indicate case of nanostructure with $f_c = 0.06\,\mathrm{nm}$, $f_e = 4.6\,\mathrm{nm}$ and $f_\kappa = f_\rho = 1.0\,\mathrm{nm}$, and solid lines indicate case of corresponding classical structure with $f_c = f_e = f_\kappa = f_\rho = 0\,\mathrm{nm}$ (color online)

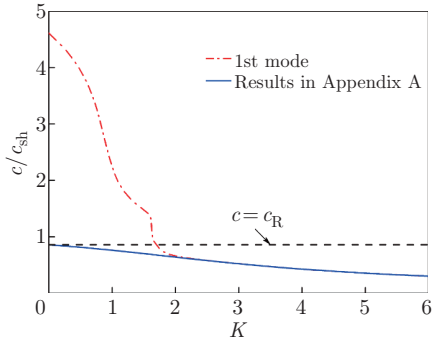

Fig. 3 Dispersion curves of 1st mode for present nanostructure and Rayleigh waves for piezoelectric half-space with surface effects (color online)

In the surface piezoelectricity theory, surface effects are characterized by several surface-related parameters. Next, the effects of these parameters upon the dispersion behaviors of

Rayleigh-type surface waves will be presented individually. In what follows, it should be noted that the 2nd mode is included to represent the high-order modes.

Dispersion curves of the lowest two modes for different f_c and f_e are illustrated in Fig. 4 and Fig. 5, respectively. Within the considered frequency range of $K < 4$, it is found from Fig. 4(a) that the surface elasticity has little effect on the phase velocity of the 1st mode at lower (about $K < 0.6$) and higher (about $K > 1.6$) frequencies, while such effect becomes significant in the other frequency range, and the stronger surface elasticity indicated by the larger value of f_c induces the higher wave velocity. A close comparison of Fig. 5(a) with Fig. 4(a) reveals that the effect of surface piezoelectricity upon the 1st mode is similar to those of the surface elasticity. For the 2nd mode shown in Fig. 4(b) and Fig. 5(b), the phase velocity is also raised due to the existence of surface elasticity or surface piezoelectricity. The cut-off frequency remains nearly constant as the f_e changes, while it grows larger with an increase in f_c, which implies the surface elastic effect can narrow the frequency range of the high-order modes.

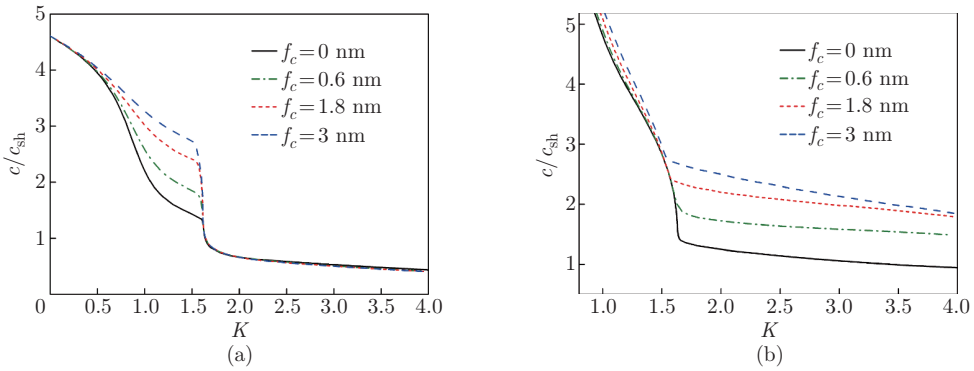

Fig. 4 Lowest two modes for different f_c ($f_e = 4.6\,\text{nm}$ and $f_\kappa = f_\rho = 1\,\text{nm}$): (a) 1st mode; (b) 2nd mode (color online)

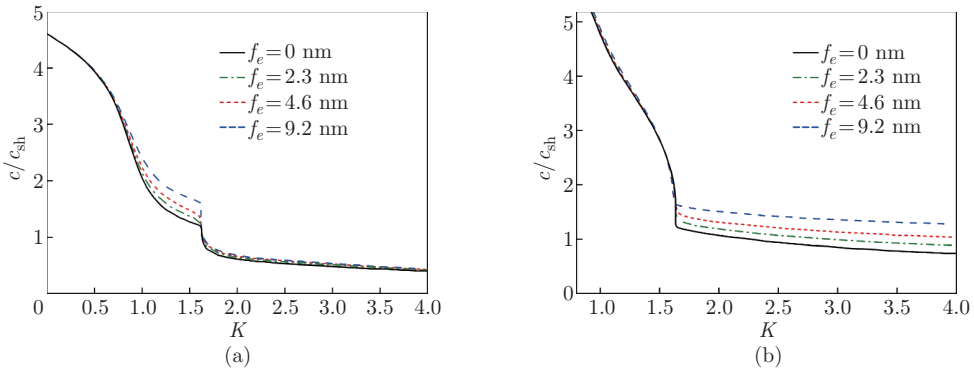

Fig. 5 Lowest two modes for different f_e ($f_c = 0.06\,\text{nm}$ and $f_\kappa = f_\rho = 1\,\text{nm}$): (a) 1st mode; (b) 2nd mode (color online)

Similar plots for different f_κ and f_ρ are given in Fig. 6 and Fig. 7, respectively. Whether the surface dielectricitiy or surface density is involved, one can note that the phase velocity decreases with increasing the corresponding surface parameters. By inspection of Fig. 6(a) and Fig. 7(a), it is observed that the change of the 1st mode resulting from the surface dielectric effect is slight in the relatively low and high frequency range, which is similar to the results in

Fig. 4(a) and Fig. 5(a); however, the presence of surface density considerably reduces the wave velocity at each nonzero frequency. In addition, Fig. 6(b) and Fig. 7(b) show that the cut-off frequency of the 2nd mode decreases significantly as the value of f_κ or f_ρ increases. Contrary to the contribution of surface elasticity shown in Fig. 4(b), this phenomenon indicates that the frequency range of the high-order modes is broadened with consideration of the surface dielectricity or surface density.

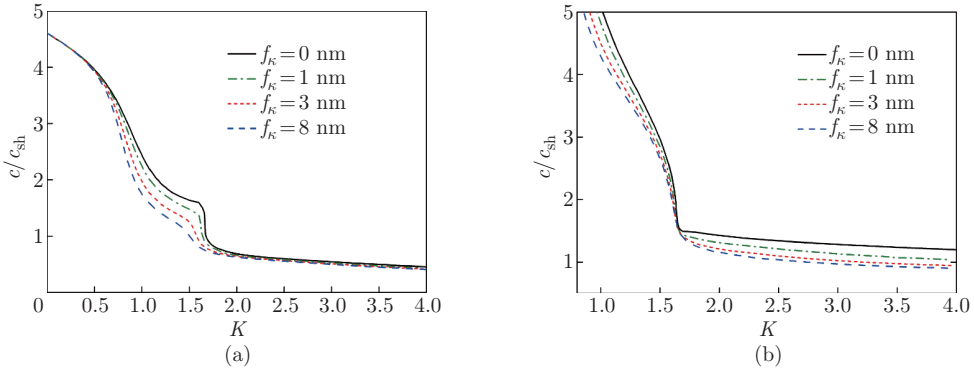

Fig. 6 Lowest two modes for different f_κ ($f_c = 0.06\,\text{nm}$, $f_e = 4.6\,\text{nm}$, and $f_\rho = 1\,\text{nm}$): (a) 1st mode; (b) 2nd mode (color online)

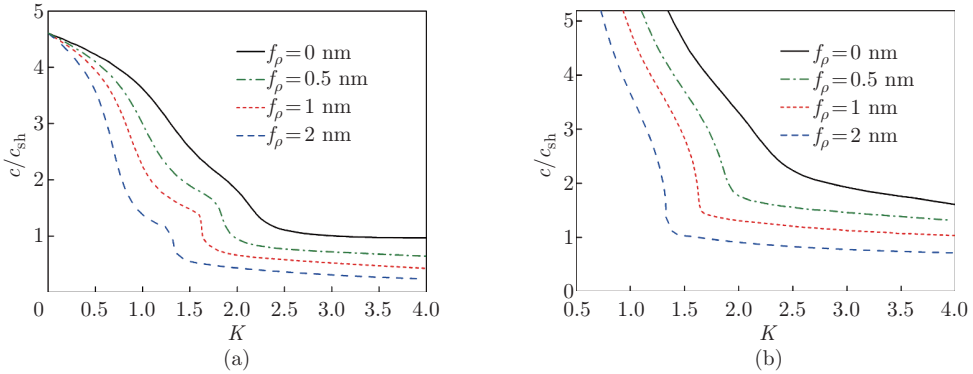

Fig. 7 Lowest two modes for different f_ρ ($f_c = 0.06\,\text{nm}$, $f_e = 4.6\,\text{nm}$, and $f_\kappa = 1\,\text{nm}$): (a) 1st mode; (b) 2nd mode (color online)

The variations of dispersion curves of the lowest three modes with different surface residual stresses are plotted in Fig. 8. For the 1st mode in Fig. 8(a), it is clear that the effect of surface residual stress on the phase velocity is very small at lower frequencies, while it becomes more pronounced as the frequency increases. Specifically, the positive surface residual stress causes the increase in phase velocity, and the larger the positive residual stress is, the higher the phase velocity is, whereas the negative surface residual stress decreases the magnitude of phase velocity, and the larger the negative residual stress is, the lower the phase velocity is. For the 2nd and 3rd modes, it is observed from Fig. 8(b) that the surface residual stress has no effect on their propagation velocity.

From the above discussion, it can be concluded that the impact of surface effects on the 1st mode is mainly characterized by the surface density at lower frequencies, while it is dominated by the surface residual stress and surface density at higher frequencies. For the high-order modes,

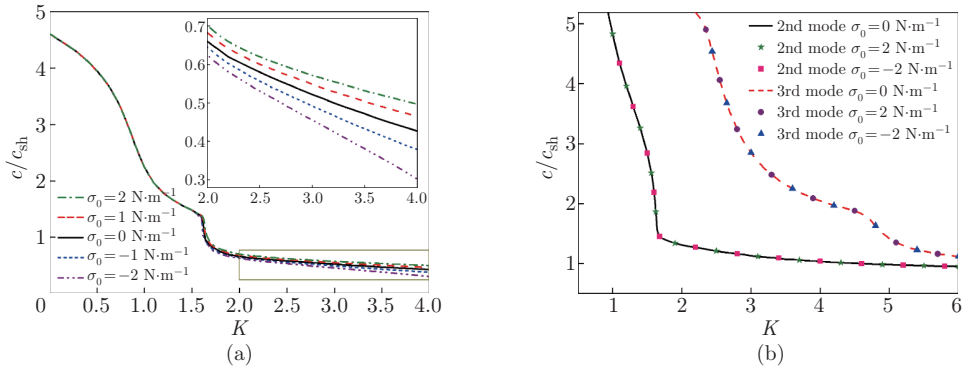

Fig. 8 Lowest three modes for different σ_0 ($f_c = 0.06\,\text{nm}$, $f_e = 4.6\,\text{nm}$, and $f_\kappa = f_\rho = 1\,\text{nm}$): (a) 1st mode; (b) 2nd and 3rd modes (color online)

the discrepancy resulting from the surface effects is completely determined by the variation of surface material properties rather than surface residual stress, and the magnitude of cut-off frequency is independent of surface piezoelectricity.

Dispersion curves of the lowest two modes for different nanofilm thicknesses are provided in Fig. 9. In particular, the results without surface effects corresponding to the classical case are also included for comparison. It is well-known that the classical dispersion behaviors for Rayleigh-type surface waves are irrelevant to the film thickness. However, as Fig. 9(a) and Fig. 9(b) suggest, the dispersion curves with surface effects exhibit obvious size-dependency, which is manifested in the variation of phase velocity for different nanofilm thicknesses under a given frequency. Moreover, it can be observed that the thinner the nanofilm is, the greater the difference is between the classical and nonclassical cases. This is consistent with the fact that the surface effects become more prominent as the size of nanostructure decreases. Instead, it is reasonably deduced from Fig. 9 that the surface effects can be ignored when the nanofilm thickness grows big enough, which implies that there exists a critical film thickness below which the surface effects should be considered.

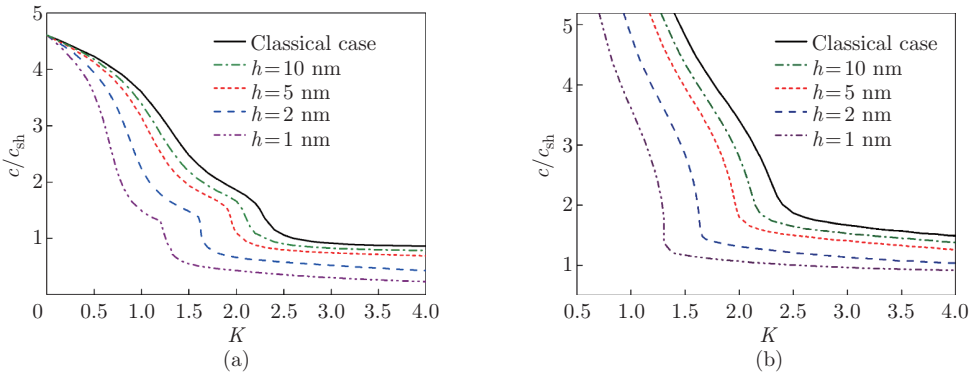

Fig. 9 Lowest two modes for different h ($f_c = 0.06\,\text{nm}$, $f_e = 4.6\,\text{nm}$, and $f_\kappa = f_\rho = 1\,\text{nm}$): (a) 1st mode; (b) 2nd mode (color online)

5 Conclusions

Based on the surface piezoelectricity theory, the dispersion properties of Rayleigh-type surface waves propagating in a layered piezoelectric nanostructure consisting of a piezoelectric nanofilm and an elastic substrate are theoretically studied in this work. The dispersion equation is derived in a concrete form, and the effects of several surface-related parameters on the dispersion modes are analyzed in detail. Analysis results reveal that the dispersion behaviors predicted by the current formulation exhibit significant differences from the classical case, which further illustrates the necessity of considering surface effects for accurately modeling the overall mechanical properties of piezoelectric nanostructures. The enhanced surface elasticity and surface piezoelectricity increase the wave velocity, while it may decrease as the surface dielectricity and surface density grow. In addition, it is observed that the surface residual stress only affects the fundamental Rayleigh mode, and the bigger positive and negative surface residual stresses result in the higher and lower phase velocities, respectively. This work is expected to be helpful for understanding the size-dependent dispersion properties of piezoelectric nanostructures and provide guidelines for the design of these nanostructures through surface engineering.

References

[1] XU, S. Y., POIRIER, G., and YAO, N. PMN-PT nanowires with a very high piezoelectric constant. *Nano Letters*, **12**(5), 2238–2242 (2012)

[2] XU, S. Y., YEH, Y. W., POIRIER, G., MCALPINE, M. C., REGISTER, R. A., and YAO, N. Flexible piezoelectric PMN-PT nanowire-based nanocomposite and device. *Nano Letters*, **13**(6), 2393–2398 (2013)

[3] XU, S., QIN, Y., XU, C., WEI, Y. G., YANG, R. S., and WANG, Z. L. Self-powered nanowire devices. *Nature Nanotechnology*, **5**(5), 366–373 (2010)

[4] WANG, X. D., SONG, J. H., LIU J., and WANG, Z. L. Direct-current nanogenerator driven by ultrasonic waves. *Science*, **316**(5821), 102–105 (2007)

[5] ZHOU, J., GU, Y. D., FEI, P., MAI, W. J., GAO, Y. F., YANG, R. S., BAO, G., and WANG, Z. L. Flexible piezotronic strain sensor. *Nano Letters*, **8**(9), 3035–3040 (2008)

[6] WU, J. M., CHEN, C. Y., ZHANG, Y., CHEN, K. H., YANG, Y., HU, Y. F., HE, J. H., and WANG, Z. L. Ultrahigh sensitive piezotronic strain sensors based on a $ZnSnO_3$ nanowire/microwire. *ACS Nano*, **6**(5), 4369–4374 (2012)

[7] TANNER, S. M., GRAY, J. M., ROGERS, C. T., BERTNESS, K. A., and SANFORD, N. A. High-Q GaN nanowire resonators and oscillators. *Applied Physics Letters*, **91**(20), 203117 (2007)

[8] TRIVEDI, S. and NEMADE, H. B. Simulation of a Love wave device with ZnO nanorods for high mass sensitivity. *Ultrasonics*, **84**, 150–161 (2018)

[9] WANG, X. D., ZHOU, J., SONG, J. H., LIU, J., XU, N. S., and WANG, Z. L. Piezoelectric field effect transistor and nanoforce sensor based on a single ZnO nanowire. *Nano Letters*, **6**(12), 2768–2772 (2006)

[10] HE, J. H., HSIN, C. L., LIU, J., CHEN, L. J., and WANG, Z. L. Piezoelectric gated diode of a single ZnO nanowire. *Advanced Materials*, **19**(6), 781–784 (2007)

[11] AGRAWAL, R., PENG, B., GDOUTOS, E. E., and ESPINOSA, H. D. Elasticity size effects in ZnO nanowires-a combined experimental-computational approach. *Nano Letters*, **8**(11), 3668–3674 (2008)

[12] CHEN, C. Q., SHI, Y., ZHANG, Y. S., ZHU, J., and YAN, Y. J. Size dependence of Young's modulus in ZnO nanowires. *Physical Review Letters*, **96**(7), 075505 (2006)

[13] DAI, S. X. and PARK, H. S. Surface effects on the piezoelectricity of ZnO nanowires. *Journal of Mechanics and Physics of Solids*, **61**(2), 385–397 (2013)

[14] HOANG, M. T., YVONNET, J., MITRUSHCHENKOV, A., and CHAMBAUD, G. First-principles based multiscale model of piezoelectric nanowires with surface effects. *Journal of Applied Physics*, **113**(1), 014309 (2013)

[15] QIAN, D. H. Electro-mechanical coupling wave propagating in a locally resonant piezoelectric/elastic phononic crystal nanobeam with surface effects. *Applied Mathematics and Mechanics* (*English Edition*), **41**(3), 425–438 (2020) https://doi.org/10.1007/s10483-020-2586-5

[16] FANG, X. Q., LIU, J. X., and GUPTA, V. Fundamental formulations and recent achievements in piezoelectric nano-structures: a review. *Nanoscale*, **5**(5), 1716–1726 (2013)

[17] YAN, Z. and JIANG, L. Y. Modified continuum mechanics modeling on size-dependent properties of piezoelectric nanomaterials: a review. *Nanomaterials*, **7**(2), 27 (2017)

[18] HONG, J., HE, Z., ZHANG, G., and MI, C. Size and temperature effects on band gaps in periodic fluid-filled micropipes. *Applied Mathematics and Mechanics* (*English Edition*), **42**(9), 1219–1232 (2021) https://doi.org/10.1007/s10483-021-2769-8

[19] GURTIN, M. E. and MURDOCH, A. I. A continuum theory of elastic material surfaces. *Archive for Rational Mechanics and Analysis*, **57**(4), 291–323 (1975)

[20] WANG, J. X., HUANG, Z. P., DUAN, H. L., YU, S. W., FENG, X. Q., WANG, G. F., ZHANG, W. X., and WANG, T. J. Surface stress effect in mechanics of nanostructured materials. *Acta Mechanica Solida Sinica*, **24**(1) 52–82 (2011)

[21] HUANG, G. Y. and YU, S. W. Effect of surface piezoelectricity on the electromechanical behavior of a piezoelectric ring. *Physica Status Solidi B*: *Basic Solid State Physics*, **243**(4) 22–24 (2006)

[22] PAN, X. H., YU, S. W., and FENG, X. Q. A continuum theory of surface piezoelectricity for nanodielectrics. *SCIENCE CHINA Physics Mechanics & Astronomy*, **54**(4), 564–573 (2011)

[23] XIAO, J. H., XU, Y. L., and ZHANG, F. C. Evaluation of effective electroelastic properties of piezoelectric coated nano-inclusion composites with interface effect under antiplane shear. *International Journal of Engineering Science*, **69**, 61–68 (2013)

[24] FANG, X. Q., YANG, Q., LIU, J. X., and FENG, W. J. Surface/interface effect around a piezoelectric nano-particle in a polymer matrix under compressional waves. *Applied Physics Letters*, **100**(15), 151602 (2012)

[25] ZHANG, L. L., LIU, J. X., FANG, X. Q., and NIE, G. Q. Size-dependent dispersion characteristics in piezoelectric nanoplates with surface effects. *Physica E*, **57**, 169–174 (2014)

[26] ZHANG, C. L., CHEN, W. Q., and ZHANG, C. On propagation of anti-plane shear waves in piezoelectric plates with surface effect. *Physics Letters A*, **376**(45), 3281–3286 (2012)

[27] YAN, Z. and JIANG, L. Y. Surface effects on the electromechanical coupling and bending behaviours of piezoelectric nanowires. *Journal of Physics D*: *Applied Physics*, **44**(7), 075404 (2011)

[28] YAN, Z. and JIANG, L. Y. The vibrational and buckling behaviors of piezoelectric nanobeams with surface effects. *Nanotechnology*, **22**(24), 245703 (2011)

[29] ZHANG, J., WANG, C. Y., and ADHIKARI, S. Surface effect on the buckling of piezoelectric nanofilms. *Journal of Physics D*: *Applied Physics*, **45**(28), 285301 (2012)

[30] ZHANG, J. and WANG, C. Y. Vibrating piezoelectric nanofilms as sandwich nanoplates. *Journal of Applied Physics*, **111**(9), 094303 (2012)

[31] LI, Y. H., FANG, B., ZHANG, J. H., and SONG, J. Z. Surface effects on the wrinkling of piezoelectric films on compliant substrates. *Journal of Applied Physics*, **110**(11), 114303 (2011)

[32] GUO, X. and WEI, P. J. Dispersion relations of in-plane elastic waves in nano-scale one dimensional piezoelectric semiconductor/piezoelectric dielectric phononic crystal with the consideration of interface effect. *Applied Mathematical Modelling*, **96**, 189–214 (2021)

[33] HUANG, Y., DAS, P. K., and BHETHANABOTLA, V. R. Surface acoustic waves in biosensing applications. *Sensors and Actuators Reports*, **3**, 100041 (2021)

[34] YANG, W. J., LIANG, X., and SHEN, S. P. Love waves in layered flexoelectric structures. *Philosophical Magazine*, **97**(33), 3186–3209 (2017)

[35] WANG, X., LI, P., and JIN, F. A generalized dynamic model of nanoscale surface acoustic wave sensors and its applications in Love wave propagation and shear-horizontal vibration. *Applied Mathematical Modelling*, **75**, 101–115 (2019)

[36] CHEN, T. Y., CHIU, M. S., and WENG, C. N. Derivation of the generalized Young-Laplace equation of curved interfaces in nanoscaled solids. *Journal of Applied Physics*, **100**(7), 074308 (2006)

[37] YANG, J. S. *Analysis of Piezoelectric Devices*, World Scientific Publishing, Hackensack (2006)
[38] BENETTI, M., CANNATA, D., DI-PIETRANTONIO, F., and VERONA, E. Growth of ALN piezoelectric film on diamond for high-frequency surface acoustic wave devices. *IEEE Transactions on Ultrasonics Ferroelectrics and Frequency Control*, **52**(10), 1806–1811 (2005)

Appendix A

Dispersion equation of Rayleigh waves in a piezoelectric semi-infinite solid is derived with considering the surface effects.

For Rayleigh waves propagating in a piezoelectric solid occupying the half-space $x_3 \geqslant 0$, the solutions to Eqs. (1)–(3) can be expressed in the following forms:

$$u_2 = \sum_{m=1}^{3} \hbar_m A_{3m} \mathrm{e}^{kb_m x_3} \mathrm{e}^{\mathrm{i}k(x_2 - ct)}, \tag{A1}$$

$$u_3 = \sum_{m=1}^{3} \overline{\lambda}_m A_{3m} \mathrm{e}^{kb_m x_3} \mathrm{e}^{\mathrm{i}k(x_2 - ct)}, \tag{A2}$$

$$\phi = \sum_{m=1}^{3} A_{3m} \mathrm{e}^{kb_m x_3} \mathrm{e}^{\mathrm{i}k(x_2 - ct)}, \tag{A3}$$

where $\hbar_m$ and $\overline{\lambda}_m$ are defined by Eq. (14), and b_m $(m = 1, 2, 3)$ obtained from Eq. (9) should be with the negative real part in view of the attenuation condition $\lim\limits_{x_3 \to +\infty} (u_2, u_3, \phi) = 0$.

Consider a piezoelectric surface adhering to the semi-infinite solid locating at the plane $x_3 = 0$, where the boundary conditions are also described by Eqs. (29)–(31). Inserting Eqs. (A1)–(A3) into Eqs. (29)–(31) yields three homogeneous equations for unknown amplitudes, and the existence of nonzero solutions requires that the determinant of the coefficient matrix must vanish, i.e.,

$$|\boldsymbol{P}| = 0, \tag{A4}$$

where $\boldsymbol{P}$ is the coefficient matrix, and

$$\begin{cases} P_{1n} = k(-c_{11}^{\mathrm{s}} \hbar_n + \mathrm{i}e_{31}^{\mathrm{s}} b_n) + c_{44} \hbar_n b_n + \mathrm{i}(c_{44} \overline{\lambda}_n + e_{15}) + \rho_{\mathrm{s}} k c^2 \hbar_n, \\ P_{2n} = -k\sigma_0 \overline{\lambda}_n + \mathrm{i}c_{13} \hbar_n + b_n(c_{33} \overline{\lambda}_n + e_{33}) + \rho_{\mathrm{s}} k c^2 \overline{\lambda}_n, \\ P_{3n} = k\kappa_{11}^{\mathrm{s}} + b_n(e_{33} \overline{\lambda}_n - \kappa_{33}) + \mathrm{i}e_{31} \hbar_n. \end{cases} \tag{A5}$$

It is evident that the phase velocity is related to the frequency in Eq. (A4), thus Rayleigh waves in a piezoelectric half-space with considering the surface effects are dispersive, and Eq. (A4) is the so-called dispersion equation. The dispersion properties characterized by Eq. (.4) are completely resulted from the surface effects, that is to say, Eq. (A4) of vanishing all surface-related parameters is independent of the frequency, and then the classical Rayleigh wave velocity c_{R} can be solved. Moreover, the surface-related parameters in Eq. (A4) are presented by multiplying the wave number k, which means that the surface effects are absent when $k \to 0$. Consequently, the phase velocity will be c_{R} if $k \to 0$, which is the same as the observation from Fig. 3.